



THE 10TH INTERNATIONAL WORKSHOP
ON ADVANCED MATERIALS
SCIENCE AND NANOTECHNOLOGY

PROCEEDINGS



PUBLISHING HOUSE FOR SCIENCE AND TECHNOLOGY
AUGUST, 2021

- 60 **Effect of TiAl target power on microstructure and mechanical behavior of sputtered TiAlCrN coatings** AEM-P16 306
Luong Van Duong, Vu Nguyen Hoang, Nguyen Ngoc Linh, Dang Quoc Khanh, and Doan Dinh Phuong

ADVANCED MATERIALS AND NANOTECHNOLOGIES FOR ENERGY, LIFE SCIENCE, AND ENVIRONMENT (ELE)

- 61 **Multicomponent metal alloys tested for hydrogen storage** ELE-K04* 312
Katarina Šušťová, Dagmara Varcholová, Zuzana Molčanová, Beáta Ballóková, Jens Möllmer, Natália Jasminská, Marian Lázár, Tomáš Brestovič, Mária Podobová, Róbert Džunda, Rastislav Motýl, and Karel Saksla
- 62 **Multifunctional nanomaterials for counting biosensor applications: synthesis and properties** ELE-I13* 319
Nguyen Hoang Nam, Phi Thi Huong, Luu Manh Quynh, Chu Tien Dung, and Nguyen Hoang Luong
- 63 **Investigation of photocatalytic NO degradation over Ag loaded TiO₂ under visible light irradiation** ELE-O08 327
Pham Van Viet, Nguyen Khanh Duy, and Cao Minh Thi
- 64 **Synthesis and structure characterization of ZnO nanorods grown on bacterial cellulose 3D scaffold** ELE-O12 332
Dao Quang Khai, Mai Hong Hanh, Dam Ngoc My, and Nguyen Hoang Duong
- 65 **Fabrication and photocatalytic property of ZnO nanorod films** ELE-P04 337
Vu Duy Thinh, Vu Dinh Lam, Ta Ngoc Bach, Phung Thi Thu, Le Thi Hong Phong, Do Hung Manh, and Ngo Thi Hong Le
- 66 **Structural analysis of polyurea used as elastomer against explosion** ELE-P07 342
C. Boonruang, K. Thumani, K. Won-in, and P. Dararutana
- 67 **Effects of chitosan-neem oil microemulsion on *Sitophilus oryzae*** ELE-P09 346
Nguyen Thi Nhu Quynh and Nguyen Thi Thanh Tam
- 68 **Acute oral toxicity and repeated dose 7-day oral toxicity study of Fe-BTC-PEG for drug delivery purpose** ELE-P11 352
Nguyen Thi Hoai Phuong, Do Thi Thao, Nguyen Que Chau, Le Thanh Bac, Nguyen Thi Phuong, Tran Van Chinh, Phung Khac Nam Ho, Le Minh Tri, and Ninh Duc Ha

*Editor's suggestion

Fabrication and photocatalytic property of ZnO nanorod films

Vu Duy Thinh^{1,2,*}, Vu Dinh Lam¹, Ta Ngoc Bach², Phung Thi Thu⁴, Le Thi Hong Phong², Do Hung Manh², and Ngo Thi Hong Le^{1,2}

¹Graduate University of Science and Technology, VAST, 18 Hoang Quoc Viet, Cau Giay, Hanoi, Vietnam

²Institute of Materials Science, VAST, 18 Hoang Quoc Viet, Cau Giay, Hanoi, Vietnam
³Hanoi University of Mining and Geology, 18 Pho Vien, Dong Ngac, Bac Tu Liem, Hanoi, Vietnam

⁴University of Science and Technology of Hanoi, VAST, 18 Hoang Quoc Viet, Cau Giay, Hanoi, Vietnam

*Email: vuduythinhbk@gmail.com

Abstract. ZnO nanorods are successfully fabricated on the FTO substrate by a simple and low-cost hydrothermal method. The structural, morphological and optical properties of the re-prepared samples are determined by X-ray diffraction (XRD), field emission scanning electron microscopy (FESEM) and fluorescence spectroscopy. The FESEM images show the predominant dependence of different morphologies on the ratio of precursors. The obtained ZnO nanorods have hexagonal structures with diameters of about 230 nm and are relatively uniform. The photocatalytic activity of ZnO films in the UVA light region is evaluated through the capability to degrade methyl orange (MO). The results reveal that the ZnO film with hexagonal rod structure has the best photocatalytic performance compared with other geometries fabricated in this work.

Keywords: ZnO nanorods, ZnO films, methylene blue, hydrothermal method, photocatalytic activity

1. Introduction

The enormous development of industry along with the population outbreak has caused severe consequences for the living environment on Earth. Among global environmental issues, water pollution is the primary concern of countries in the world because many water bodies are now seriously polluted due to toxic chemicals and dyes from sewage. This leads to vast damage or even ruin aquatic life and human health. Various physical and chemical methods have been proposed and studied in several decades in order to deal with these issues. Most typically, photocatalytic degradable technology is one of the most promising approaches in the water treatment strategy because it is known as a low-cost, environmentally-friendly and sustainable technology, which produces none of secondary pollution [1]. In this regard, an ideal catalyst should have an excellent efficiency, a large specific surface under the sunlight, and recyclability [1].

Along with the challenges in the consecutively developing process of photocatalytic technology, a range of various photocatalysts, such as TiO₂, Bi₂O₃, Fe₂O₃, CdS, metal-organic framework, CuO, carbon materials and their compounds, has been reported [2–6]. Among the excellent photocatalysts, ZnO has emerged as a greatly potential catalyst, which is strongly active in the ultraviolet light region,

thanks to its outstanding properties, for instances, direct band gap of 3.2 eV, large binding energy of 60 meV, nontoxicity, high temperature and chemical stability and low cost [7]. Nevertheless, one of the major impediment, which stems from its large band gap, is the decrease of photocatalytic reaction. To overcome this drawback, different modifications, such as doping, noble metal decoration and composite have been investigated [5,8,9]. On the other hand, the changes of size and morphology of materials may modify chemical and physical characteristics. Consequently, photocatalytic properties of materials can be improved [10] without doping other materials. As shown in reports, depending on the used precursors and their concentrations, the solvents, the pH of the solution, and synthesis methods and their conditions, ZnO can be synthesized into various morphologies with high surface area, such as nanorods, nanowires and flower-like shape [11]. Recently, ZnO film fabricating technology has received much attention because of its practical application. However, the photodegradation time of ZnO films has still been an issue, which needs to be solved. A variety of fabricating techniques has been explored, such as sol-gel spin coating [12], spray pyrolysis [13], dip coating [14], radio frequency magnetron sputtering [15] and hydrothermal method [16].

In this work, nanostructured ZnO films were prepared on the FTO (F:SnO₂) using hydrothermal method at reasonable conditions. In addition to discussion of structure and optical characteristics of ZnO films, we analyzed the impact of precursor molar concentration on their morphology and photocatalytic degradation process. This study contributes to enhance the practical application capacity of nanostructured ZnO materials.

2. Experimental

2.1. Synthesis and characterization

All reagents including zinc acetate dihydrate (Zn(CH₃COO)₂·2H₂O), zinc nitrate hexahydrate (Zn(NO₃)₂·6H₂O) and ethanol were commercially purchased from Sigma-Aldrich with high purity. To synthesize ZnO film on FTO (F:SnO₂), the commercial FTO substrate with the surface area of 4 cm² was first pre-treated by distilled water and ethanol and then dried. Subsequently, 1 g zinc nitrate hexahydrate was dissolved in 50 ml ethanol under stirring until obtaining a homogeneous solution at room temperature. Next, this solution was utilized to create one initial layer on the FTO substrate by using spin coating and after that, it was heated at 120 °C for 1 hour. The obtained film together with zinc acetate solution of variable molar concentration (C_M = 0.01M, 0.0075M, 0.005M and 0.002M and denoted as Z0.01, Z0.0075, Z0.005 and Z0.002, respectively) was introduced into a Teflon autoclave and kept at 90 °C for 8 hours. When the experiment ended, the substrate was taken out and rinsed with distilled water several times and then dried in an oven at 70 °C overnight.

The morphology of all samples was observed by Hitachi s-4800 field emission scanning electron microscopy (FESEM). The crystal structure was obtained by a Bruker D8 advanced X-ray power diffractometer with Cu-Kα radiation. The photoluminescence (PL) spectrum was measured by iHR550 high resolution PL spectroscopy. The UV-vis adsorption spectrum was examined by an UV-vis spectrophotometer Carry 5000.

2.2. Photocatalytic test

The photocatalytic efficiency of ZnO film was examined through the degradation of methyl orange (MO) concentration under Xenon lamp (Solar Simulator: Oriel SolIA 100mW/cm²), which simulates the sunlight. Typically, the as-prepared ZnO film was soaked into 50 ml of MO solution (C_M = 2 ppm) in a beaker. The photocatalytic test was carried out at room temperature and pH = 7 after the MO solution and ZnO film had kept together in the dark for 60 min at 300 rpm to reach adsorption desorption equilibrium. Each 3 ml MO solution was taken out in every 1 hour interval to study the adsorption spectra. Carry 5000 device was applied to analyze the dye photodegradation by means of the change of the absorption spectrum intensity of MO at the wavelength of 655 nm.

3. Results and discussion

The FESEM images of as-prepared ZnO films are shown in Fig. 1. In particular, a hexagonal column-like shape is observed in the sample with the lowest amount of zinc acetate, while it is not introduced in the others. The diameters of these hexagonal columns are approximately 120 nm and the length of those are around several micrometers. The significant change of morphology is pointed out when increasing

the zinc acetate amount from 0.002 to 0.01 M. It can be seen obviously that the wall of rod is formed first and then the core is gradually filled via the increase of precursor concentration. Therefore, Z0.005 sample has hollow rod shape while the remaining two samples show fulfilled rods, nonetheless they have interlocking trend. The results clearly unveil that the zinc acetate concentration works as a key parameter in the development of geometric structure of ZnO.

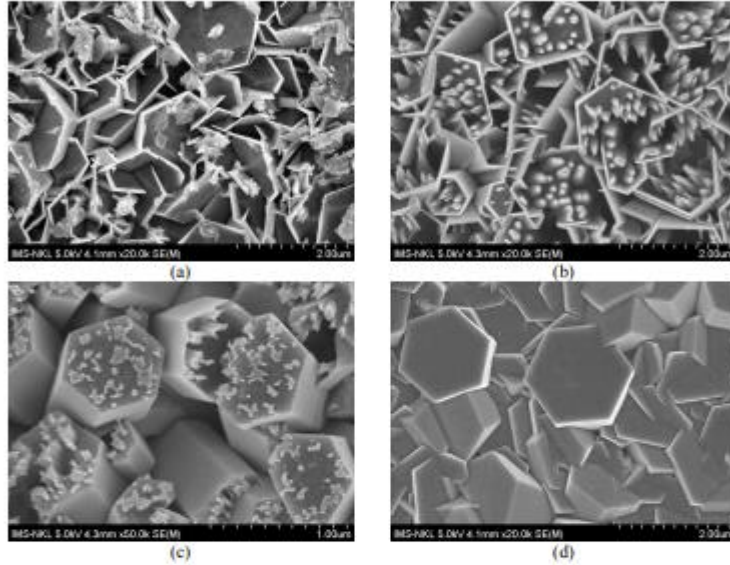


Figure 1. FESEM images of ZnO films synthesized at the different molar of Zn precursor: (a) Z0.002, (b) Z0.005, (c) Z0.0075 and (d) Z0.01.

The crystal structure information of Z0.002, Z0.005, Z0.0075 and Z0.01 samples is determined by X-ray diffraction pattern. As shown in Fig. 2, diffraction peaks of the samples appear around $2\theta \approx 31.8^\circ$, 34.5° , 36.34° , 47.6° , 56.6° and 62.9° corresponding to (100), (002), (101), (102), (110) and (103) planes, respectively. This result is in good agreement with the 36-1451 JCPDS reference and concurrently confirms that all synthesized ZnO films have a hexagonal wurtzite crystal structure. Furthermore, from the XRD pattern, it can be confirmed that the formation of c-axis oriented ZnO nanorods grown on the FTO can be deduced from strong (002) diffraction peak. [17].

Figure 3 plots the room-temperature PL spectra of ZnO films by the exciting source of Laze Team Phonic 355 nm. The PL spectra of all samples consist of one band with high intensity in the UV region and one wide band in the visible. The former is characteristic for ZnO due to recombination of free excitons, bound excitons and transition in the donor-acceptor pairs [18]. The latter can be due to the presence of defects in the ZnO films. The MO degradable efficiency of ZnO films is calculated by equation:

$$C(\%) = \frac{C_0 - C_t}{C_0} \times 100,$$

where C_0 and C_t are the concentrations of MO solutions before and after irradiation at time t , respectively. Similar to the morphology, the MO degeneration rate of ZnO film depends on the precursor concentration, as shown in Fig. 4. Particularly, the one with the zinc acetate concentration of 0.005

exhibits the highest photocatalytic activity. Specifically, about 95%, 85.2%, 65.1% and 35% MO dye are treated after 4 hours exposing under the light when using Z0.005, Z0.002, Z0.0075 and Z0.01, respectively.

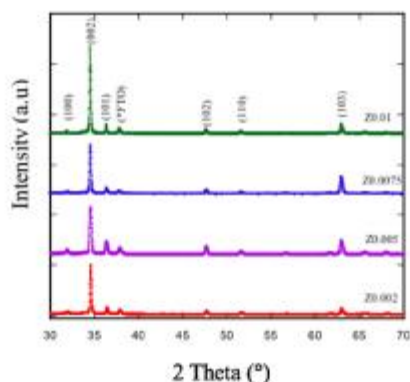


Figure 2. X-ray diffraction pattern of the prepared ZnO films.

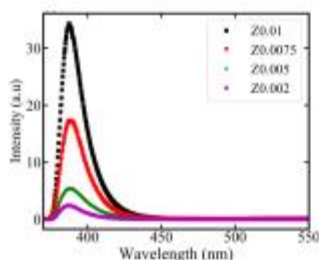


Figure 3. Photoluminescence spectra of the ZnO films grown on FTO substrate by hydrothermal method.

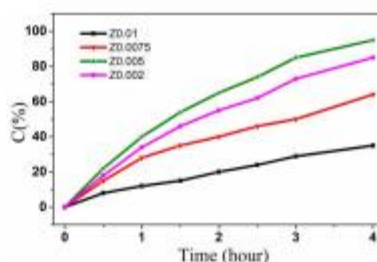


Figure 4. The dye photodegradable performance of different ZnO films with respect to time.

The underlying photocatalytic mechanism of semiconductors as ZnO, was represented in detailed elsewhere [19, 20]. When being irradiated by light with energy higher or equal to the band gap of ZnO, electrons in the valence band will be excited to the conduction band, giving rise to the generation of holes in the valence band. Both photogenerated carriers, which are electron and hole, emigrate separately to the photocatalyst's surface and take part in oxidation and reduction reactions. The reaction between the electron and oxygen on the surface of ZnO will produce superoxide radicals. Whereas, the holes can react with water to form hydroxyl radicals. Both radicals will involve in the MO decomposing process.

4. Conclusion

We successfully synthesized and studied the influence of precursor concentration on the morphology, crystal structure, optical and photocatalytic characteristics of the ZnO film. The increase of zinc acetate amount results in the change of morphology of ZnO from the hexagonal column-like rods to unperfected rods. The difference in the morphology plays an important key in the enhancement of the

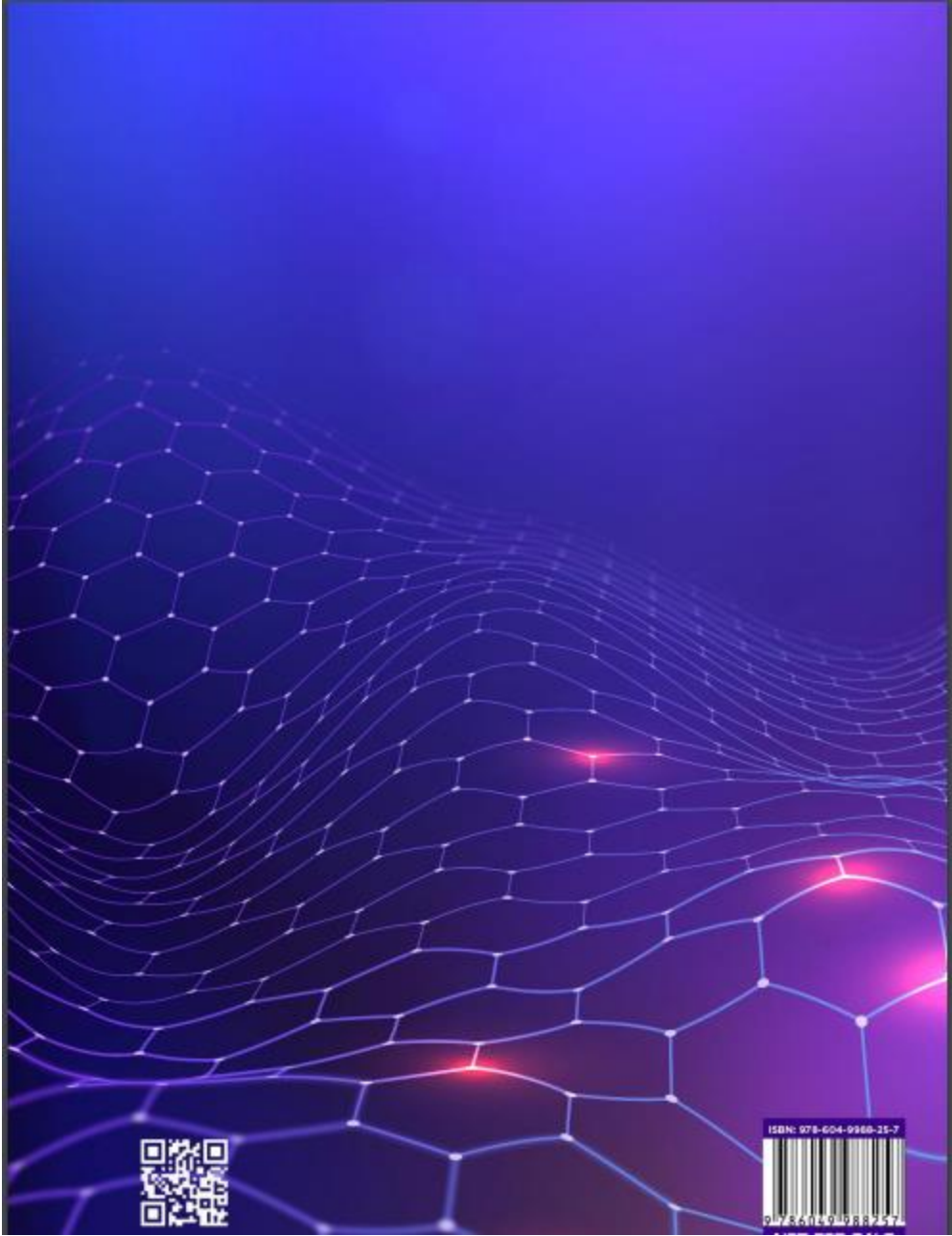
photodegradable rate as well as the reaction yield. With the hollow rod structure, Z0.005 exhibited better photocatalytic efficiency, which is attributed to the larger surface area compared to the other samples. More noticeably, the ZnO films can be reused easily without encountering problems when using ZnO nanostructure powder. These findings pave the way for further practical applicability of ZnO nanostructures, typically ZnO film.

Acknowledgments

This research was supported by the National Foundation for Science and Technology Development (NAFOSTED) under Grant No. 104.03-2017.40.

References

- [1] Zhang F, Wang X, Liu H, Liu C, Wan Y, Long Y and Cai Z 2019 *Appl. Sci.* **9** 2489.
- [2] Molina-Reyes J, Romero-Moran A, Uribe-Vargas H, Lopez-Ruiz B, Sanchez-Salas JL, Ortega E, Ponce A, Morales-Sanchez A, Lopez-Huerta F and Zuniga-Islas C 2020 *Catalysis Today* **341** 2-12.
- [3] Sanchez-Martinez D, Juarez-Ramirez I, Torres-Martinez L M and de Leon-Abarte I 2016 *Ceram. Int.* **42**(1) 2013-2020.
- [4] Joya MR, Ortega J B, Malafatti JOD and Paris EC 2019 *ACS Omega* **4**(17) 17477-17486.
- [5] Nguyen TB, Phung TT, Ngo THL, Lam TKG, Nguyen TH and Tran DL 2015 *Int. J. Nanotechnol.* **12** 447.
- [6] Matos J, Poon PS, Montana R, Romero R, Gon GR, Calves MA, Schettino JR, Passamani EC and Freitas JCC 2020 *Catalysis Today* **356** 226.
- [7] Wang ZL 2004 *J. Phys. Condens. Matter* **16**(25) R829.
- [8] Caregnato P, Jimenez KRE and Villabril PI 2021 *Catalyst Today* **372** 183-190.
- [9] Chankhanittha T, Komchoo N, Senasu T, Priyanon J, Youngme S, Herravibool K and Nanan S 2021 *Colloids. Surf. A: Physicochemical and Engineering Aspects* **626** 127034.
- [10] Samadi M, Zirak M, Naseri A, Kheirabadi M, Ebrahimi M and Moshfegh AZ 2019 *Res. Chem. Intermed.* **45** 2197-2254.
- [11] Ferreira SH, Morais M, Nunes D, Oliveira MJ, Rovisco A, Pimentel A, Aguas H, Fortunato E and Martins R 2021 *Materials* **14** 2385.
- [12] Nimbalkar AR and Patil MG 2017 *Physica B: Condensed Matter* **527** 7-15.
- [13] Mucharweni E, Sathiaraj TS and Nyakoty H 2017 *Heliyon* **3**(4) e00285.
- [14] Kaneva NV and Dushkin CD 2011 *Bulg. Chem. Commun.* **43**(2) 259-263.
- [15] Nunes P, Costa D, Fortunato E and Martins R 2002 *Vacuum* **64**(3-4) 293-297.
- [16] Gerbreders V, Krasovska M, Sledzevskis E, Gerbreders A, Mihailova I, Tamanis E and Ogurcovs A 2020 *Cryst. Eng. Comm* **22**(8) 1346-1358.
- [17] Shimpi NT, Rane YN, Shende DA, Gosavi SR and Ahirao PB 2020 *Optik* **217** 164916.
- [18] Kapustianyk V, Turko B, Rudyk V, Rudyk Y, Rudko M, Panasiuk M and Serkiz R 2016 *Opt. Mater.* **56** 71-74.
- [19] Moore JC, Louder R and Thompson CV 2014 *Coatings* **4**(3) 651-669.
- [20] Toporovska LR, Hryzak AM, Turko BI, Rudyk VP, Tsybul'skiy VS and Serkiz R 2017 *Opt. Quantum Electron.* **49**(12) 408.



ISBN: 978-604-9988-25-7



